Comparative *ab initio* study of the structural, electronic, and magnetic trends of isoelectronic late 3*d* and 4*d* transition metal clusters

F. Aguilera-Granja
Instituto de Física, Universidad Autónoma de San Luis Potos, San Luis Potosí 78000, Mexico

A. García-Fuente and A. Vega
Departamento de Física Teórica, Atómica y Óptica, Universidad de Valladolid, Valladolid 47005, Spain
(Received 29 January 2008; revised manuscript received 12 September 2008; published 29 October 2008)

We present a density-functional comparative study of the electronic properties and the structural trends of the late isoelectronic 3*d* (Fe, Co, Ni) and 4*d* (Ru, Rh, Pd) free-standing transition metal clusters of 13 and 23 atoms. Different types of structures have been analyzed: compact arrangements such as icosahedral shape, open arrangements such as the cubic ones, and structures reminiscent of the crystal lattices. We have calculated total-energy differences between the structural and the spin isomers, as well as the electronic charge and spin-moment distribution within the clusters. We have found that some structural trends correlate with electronic trends, which are consistent with the spectrum of the single atoms in the $d^n s^1$ configuration ($n=7,8,9$ for Fe and Ru, Co and Rh, and Ni and Pd, respectively). We have also found that magnetism plays a role in the Fe clusters. The exceptions found in some clusters, which depart from the structural trend obtained for their respective 3*d* or 4*d* family, illustrate the complexity of the bond formation in transition metal systems in which the itinerant but localized *d* electrons coexist with the delocalized *sp* electrons in the valence states.

DOI: 10.1103/PhysRevB.78.134425 PACS number(s): 75.75.+a, 36.40.Cg, 75.50.−y, 61.46.Bc

I. INTRODUCTION

Free-standing transition metal (TM) clusters are a subject of intense research nowadays, devoted to a great extent to the understanding of the geometrical and electronic properties at the nanoscale as well as their interplay. This knowledge is also relevant if those systems are going to be used in nanotechnology, for instance, in magnetic and/or catalytic devices in which the morphology plays a fundamental role. From the experimental side, the production of size-selected free-standing clusters in cluster beams is well controlled at present, and for instance, the magnetic properties as a function of cluster size can be investigated through Stern-Gerlach techniques.[1–3] Other electronic properties can be also characterized such as optical properties or ionization potentials. However, the geometrical structures of free-standing clusters are more difficult to be characterized since most of the techniques used in bulklike systems are not suitable if the cluster is not supported on a matrix. Therefore, in the free-standing environment, alternative ideas have emerged to find the plausible geometries. In this respect and in close connection with catalysis, it is possible to take advantage of the structural dependence of the adsorption of light molecules on the surface of the cluster.[4]

From the theoretical side, the coexistence of itinerant *d* electrons with delocalized *sp* electrons in the valence of the transition metals makes it difficult to treat them within simple models. The tight-binding approach has been extensively used for the study of the electronic structure and related magnetic properties of 3*d* and 4*d* TM clusters.[5–9] However, if the determination of both the geometry and electronic structure is being achieved at the same level, which is desirable due to the strong interdependence of both properties, density-functional theory (DFT) has been demonstrated to be a very efficient and reliable approach. Quite interesting studies in this context have been reported in the literature.[10–14] These are some examples since it would be very difficult to quote all the contributions.

Despite the very interesting results reported about the properties of clusters of particular elements, comparative studies of the general trends within the same period or group of the Periodic Table are much less often reported,[15–20] the work by Reddy *et al.*[15] being one of the pioneers in this kind of attempt. In our opinion, it would be very desirable to understand for instance why the geometrical trends in TM clusters change so dramatically in some cases as moving within the Periodic Table, despite the fact that their respective bulks may have the same structure. Of course this is a huge task if a single full systematic study is envisaged, but there exist at present enough capabilities to start shedding some light on this question. In a recent work, Wang and Johnson[20] reported an interesting comparative study of the structural trends for late TM 13-atom clusters using DFT with the generalized gradient approximation (GGA) and first-principles molecular dynamics with a thorough structural sampling. In particular these authors studied free-standing clusters of Pt, Pd, and Rh, and they explained their structural trends in terms of hybridization effects. These kind of effects were also used to explain the planar geometries of small Au clusters (in comparison for instance with Ag and Cu clusters) by Bonacić-Koutecký *et al.*,[21] Hakkinen *et al.*,[22] and Fernández *et al.*[23] This mechanism was reviewed by Agraït *et al.*[24] Gold has been itself the subject of intense research in this respect, and relativistic effects seem to govern the degree of hybridization between the localized and the delocalized states.

Our present work is devoted to a comparative study of the interplay between the electronic structure and the geometrical trends of late isoelectronic 3*d* [ferromagnetic (FM)] and 4*d* TM clusters. This comparative study has not yet been

performed and relativistic effects are expected to be less important in 3*d* than in 4*d* or 5*d* systems. We will analyze if the hybridization effects are also in this case the key for governing the geometrical trends (as it was the case in Au clusters) and which is the role played by magnetism. Two cluster sizes have been selected for this study: the 13-atom clusters and the 23-atom clusters of the 3*d* elements Fe, Co, and Ni, and their isoelectronic 4*d* Ru, Rh, and Pd. We wanted to analyze the structural trends for different sizes in order to have more data and information on the size dependence and to extract general trends. The size of 13 atoms has been studied extensively in free-standing clusters due to its having been found as a magic number for a large variety of elements. The size of 23 atoms is the lowest one that can accommodate a double icosahedron, as well as other symmetries studied also for the 13-atom clusters. In Sec. II we will describe the DFT approach used for this study and in Sec. III the results are discussed in detail. We end with a summary of the main conclusions.

II. THEORETICAL MODEL

We have performed our calculations using the DFT pseudopotential code Spanish Initiative for Electronic Simulation of Thousand of Atoms (SIESTA).[25] This method employs linear combination of pseudoatomic orbitals as basic sets. The atomic core is replaced by a nonlocal norm-conserving Troullier-Martins[26] pseudopotential that is factorized in the Kleinman-Bilander form[27] and may include nonlinear core correction terms to account for the significant overlap of the core charges with the valence *d* orbitals. The code allows performing, together with the electronic calculation, structural optimization using a variety of algorithms.

In the present calculation, we have used for the exchange and correlation potential the GGA as parametrized by Perdew *et al.*[28] The ionic pseudopotentials were generated using the following atomic configurations: $3d^n$, $4s^1$, and $4p^0$ for the 3*d* elements and $4d^n$, $5s^1$, and $5p^0$ for the 4*d* elements with $n=7$ for Fe and Ru, $n=8$ for Co and Rh, and $n=9$ for Ni and Pd. The *s*, *p*, and *d* cutoff radii were 2.00, 2.00, and 2.00 a.u. for Fe and Co; 2.05, 2.05, and 2.05 a.u. for Ni; 2.40, 2.40, and 1.70 a.u. for Ru and Rh; and 2.30, 2.46, and 1.67 a.u. for Pd. We have included nonlinear core corrections with a matching radius of 0.70 a.u. in Fe, 0.75 a.u. in Co, 0.80 a.u. in Ni, 1.40 a.u. in Ru, and 1.2 a.u. in Rh and Pd. We have tested that these pseudopotentials reproduced accurately the eigenvalues of different excited states of the respective isolated atoms. In the case of the 4*d* elements, having harder core than their 3*d* counterparts, we further refined the cutoff radii by taking them a bit closer to the maxima of the radial wave functions. This provided a slight improvement in the description of the atomic excited states.

Concerning the basis set and the energy cutoff to define the real-space grid for numerical calculations involving the electron density, a detailed and careful test has been performed. We have described the valence states using double-zeta polarized (DZP) basis sets with two orbitals having different radial forms to describe both the 4*s* (5*s*) and the 3*d* (4*d*) shells of the 3*d* (4*d*) elements and one orbital to describe the 4*p* (5*p*) shell. We tested for Fe_{13} and Ru_{13} a triple-zeta double-polarized (TZDP) basis, that is, with three radial functions per angular momentum (instead of two as in the DZP), as well as with double polarization of the valence *s* states (instead of single polarization as in the DZP). As regard to the differences of binding energy of the isomers with respect to the most stable one, we found that the TZDP leads in general to slightly lower energy differences than the DZP (in no more than 9 meV for Fe and 15 meV for Ru) and that the energetic ordering of the different isomers did not change. Concerning the interatomic distances, we found that the TZDP basis leads to slightly shorter interatomic distances and shorter average distance than the DZP basis (in no more than 0.02 Å for both Fe and Ru). We have considered an electronic temperature of 25 meV and a 250-Ry energy cutoff to define the real-space grid for numerical calculations involving the electron density. We have tested larger cutoffs and lower electronic temperature for particular cases and verified that they do not substantially modify the results.

To optimize the geometrical structures we have performed a local relaxation using the conjugate gradient algorithm, starting from a variety of initial structures with different symmetries and different spin configurations. The structural optimization was stopped when each force component at each atom in the cluster was smaller than 5 meV/Å.

Magnetic interactions in Fe and Co are quite complex. In a recent work by Rollmann *et al.*,[29] *ab initio* total-energy calculations of small Fe clusters (up to 15 atoms) were performed to show that the relaxation of the structures leads to arrangements that restores collinearity of the magnetic moments of all clusters considered so far. In a recent work, Longo *et al.*[30] using the same theoretical approach as in the present work, performed calculations for a typical Fe cluster in which noncollinear magnetic moments could be found (Fe_6 with octahedral structure) as part of a more general study on Fe-Mn clusters. All possible spin isomers were tested. The most stable isomer was found to have a distorted octahedral geometry, FM order, and a total magnetic moment of $20\mu_B$ in keeping with other authors. The most stable isomer of Fe_6 is followed by three isomers of similar octahedral geometry: two FM isomers with total magnetic moments of $18\mu_B$ and $22\mu_B$, in keeping also with other authors, and an antiferromagnetic isomer with a binding energy much lower than that of the ground state. Noncollinear structures were not found, in agreement with Rollmann *et al.*[29] In view of the above results, collinear magnetic structures are expected, not only in Fe clusters but also in clusters of 3*d* elements in the hard ferromagnetism limit that is close to the magnetic saturation (Co and Ni). For this reason we have done the calculations in the collinear framework.

III. RESULTS

In Figs. 1 and 2, we show the geometrical shapes obtained for the structural isomers investigated for clusters of Fe, Co, Ni, Ru, Rh, and Pd of $N=13$ and $N=23$, and the nomenclature used in this work, respectively. These types of structures have been reported in the literature for clusters of different elements, and among them, we can find compact arrange-

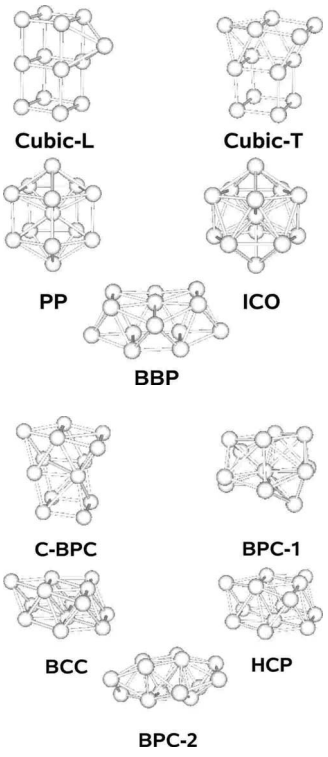

FIG. 1. Structural shapes of the isomers of clusters with 13 atoms. We have different cubic isomers (cubic-L, cubic-T, C-BPC), icosahedral (ICO), pentagonal prism (PP), buckled biplanar (BBP), different compact biplanar (BPC-1, BPC-2), fragment of body-centered cubic (bcc), and fragment of hexagonal-closed packed (hcp).

ments such as the icosahedral (ICO) ones, open arrangements such as the cubic ones, and structures reminiscent from the crystal lattices. We have not plotted the structure of each particular isomer since it is difficult to discriminate (given a structural shape) the differences between the clusters of different elements, an exception being Ru. In Ru clusters, structural deformations are present, particularly for equatior pentagonal prism (EQ-PP), equatior icosahedral (EQ-ICO), and twined icosahedral (TW-ICO), leading to wider distances distribution as compared with clusters of the other elements. In the isomer cubic of Ru_{23} structural disorder is also observed, whereas in Pd_{23} and Rh_{23} the cubic symmetry is better defined. This is illustrated in Fig. 3.

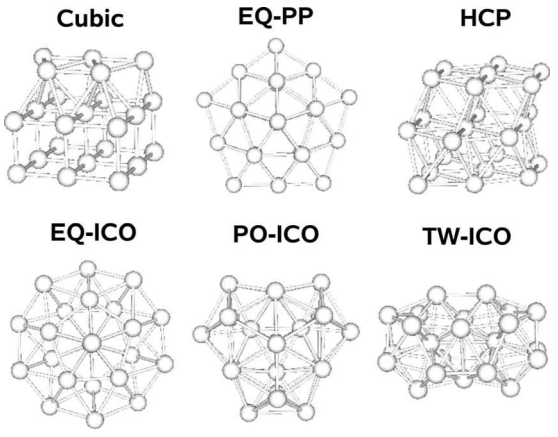

FIG. 2. Structural shapes of the isomers of clusters with 23 atoms. We have cubic isomers (cubic), equatior pentagonal prism (EQ-PP), fragment of hexagonal-closed packed (hcp), equatior icosahedron (EQ-ICO), poli icosahedron (PO-ICO), and twined icosahedron (TW-ICO) formed from two 13-atom icosahedra joined though a triangular face.

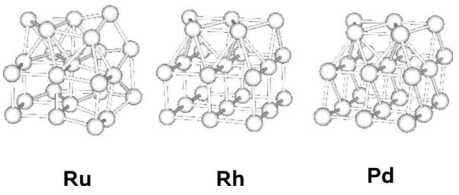

FIG. 3. Comparison of the cubic isomers of 23 atoms of Ru, Rh, and Pd. Notice the deformation of the cubic Ru_{23} and the compacity (more bonds) of the cubic Pd_{23}.

In Tables I–IV we report relevant data obtained for the different isomers of the 3*d* and 4*d* clusters. We give the total energy relative to that of the most stable isomer, average magnetic moment per atom, dipole, electronic occupations, and structural parameters. The following general trends can be inferred from the results:

(i) Compact arrangements of atoms are preferred by the 3*d* Fe and Ni clusters, as indicated by the stability of the icosahedral structures, which are, among those investigated, the ones with the larger number of bonds. For Co, the hexagonal-closed-packed (hcp) isomer, reminiscent from its bulk structure, is more stable although in Co_{23} the icosahedral structure is only 15 meV/atom less stable.

(ii) The average spin-magnetic moment per atom is similar in the different isomers of each 3*d* cluster. For instance, all Fe_{13} isomers have about $3\mu_B$/atom, those of Co_{13} have about $2\mu_B$/atom, those of Ni_{13} about $(0.6–0.9)\mu_B$/atom, and similar values for the 23-atom clusters are also obtained.

(iii) Open arrangements of atoms are preferred by the Ru and Rh clusters of both 13- and 23-atom sizes, as indicated by the stability of the cubiclike structures (cubic-T, cubic-L, and cubic), which are, among those investigated, the ones with lower number of bonds (or with the lower coordination number). An important exception of this trend within the 4*d* clusters is Pd for which the cubiclike structures are the less stable ones (cubic-L, cubic-T for $N-13$, and cubic for $N=23$).

(iv) A noticeable dispersion is obtained for the average magnetic moment per atom in different isomers of each 4*d* cluster, particularly for those of 13 atoms. Thus, we find average moments in Ru_{13} isomers within the range $(0.15–1.69)\mu_B$/atom, for Rh_{13} within $(0.69–1.62)\mu_B$/atom, and for Pd_{13} isomers within $(0.31–0.62)\mu_B$/atom. This trend can be inferred as well from the results reported by other authors in the literature for the 4*d* TM clusters.[14–20,34,35,37]

Before entering in the details of the discussion, it is worthwhile to place the above general trends in the context of previous studies reported in the literature. For Fe, Co, and Ni clusters with 13 and 23 atoms, icosahedral geometries have been suggested as the lower-energy states by different authors.[6,7,13,29,31,32] The magnetic moments reported qualitatively agree in general, although a moderated dispersion is

TABLE I. Results for the different Fe_{13}, Co_{13}, and Ni_{13} isomers. Energy difference with respect to the ground-state isomer in units of meV/atom (values in parentheses for the paramagnetic states); average magnetic moments per atom in units of μ_B; electric dipole moment in units of $e^- \times$ a.u.; per atom *sp* and *d* occupations (values in parentheses for the paramagnetic states); average nearest-neighbor distance and range of interaction distances in angstroms; and the total number of bonds considering a tolerance of 15% with respect to the bulk distances.

Structure	ΔE_B		μ	Dipole	*sp*	*d*	Distances	Bonds
Fe								
ICO	0	(90)	3.38	0.01	1.31(1.08)	6.69(6.92)	2.57,2.38–2.73	42
PP	76	(85)	3.08	0.10	1.21(1.08)	6.79(6.92)	2.53,2.38–2.76	37
BPC-1	97	(34)	3.23	0.13	1.25(1.07)	6.75(6.93)	2.58,2.32–2.99	36
BBP	108	(54)	3.08	0.13	1.22(1.08)	6.78(6.92)	2.52,2.32–2.81	36
bcc	116	(0)	3.08	0.09	1.23(1.08)	6.77(6.92)	2.57,2.33–2.97	39
hcp	129	(1)	3.23	0.06	1.26(1.08)	6.74(6.92)	2.53,2.37–2.80	36
Co								
hcp	0	(0)	2.08	0.07	1.20(1.08)	7.80(7.92)	2.42,2.32–2.52	36
BBP	47	(45)	1.92	0.08	1.11(1.09)	7.89(7.91)	2.42,2.32–2.61	36
ICO	68	(19)	2.39	0.00	1.21(1.07)	7.79(7.93)	2.49,2.39–2.55	42
PP	87	(25)	2.08	0.04	1.18(1.08)	7.82(7.92)	2.44,2.30–2.64	37
C-BPC	113	(31)	2.08	0.20	1.19(1.08)	7.81(7.92)	2.44,2.24–3.01	32
Ni								
ICO	0	(0)	0.62	0.01	1.09(1.08)	8.91(8.92)	2.47,2.38–2.53	42
BPC-2	25	(93)	0.92	0.05	1.15(1.09)	8.85(8.91)	2.44,2.35–2.96	36
BBP	30	(69)	0.77	0.08	1.12(1.09)	8.88(8.91)	2.44,2.33–2.64	36
hcp	37	(62)	0.92	0.01	1.15(1.08)	8.85(8.92)	2.46,2.37–2.59	36
PP	43	(46)	0.62	0.01	1.09(1.07)	8.91(8.93)	2.43,2.34–2.49	37

presented depending on the model and/or approximation used, the dispersion not exceeding about 25% of the larger value of the respective reported magnetic moments. Our results are consistent with previous studies except in Co_{13} for which we obtain the hcp structure (also in Co_{23} although in this case the hcp and poli icosahedron (PO-ICO) structures are nearly degenerated). The hcp structure of Co_{13} has been also found by other authors with a tight-binding approach.[33] In the case of the 4*d* clusters, there is a more complex scenario. 13-atom clusters of Pd, Rh, and Ru with radial-relaxed octahedral and icosahedral shapes were investigated more than ten years ago by Reddy *et al.*[15] who concluded that icosahedral structures were more stable than octahedral ones and that these clusters were magnetic. Other structural shapes were tested after this work. For Rh_{13} and Ru_{13}, early calculations suggested an icosahedral ground state[8,10,34] or a fragment of the fcc crystal[18,35] or even a cagelike configurations.[36] Later, a compact biplanar structure was also proposed as the possible ground state.[17] However, recent works support the cubiclike structures as the most probable ones[20,37,38] such as in our calculations. For Pd_{13}, recent calculations using Vienna Ab Initio Simulation Package (VASP) (Ref. 17) suggested a compact biplanar structure as the ground state,[17] while SIESTA, as well as other DFT approaches using ultrasoft pseudopotentials,[9,14,19] give the icosahedral structure. For Pd_{23} the polyicosahedron is the most probable ground-state structure. But in Pd several isomers are very close in energy and make of this case a very complex scenario. As regard to the magnetic moments, when the comparison is possible, our results are in keeping with other works, and as already indicated, larger dispersion in the results than for the 3*d* clusters is reported in general.

Let us discuss in more detail the trends obtained and summarized in points (i)–(iv). As indicated in Sec. I, hybridization effects have been proposed as the origin of the planar structures obtained for small Au clusters in comparison with the compact structures of their isoelectronic counterparts (Ag and Cu clusters). Relativistic effects played an important role on the relative position of the localized and delocalized states and thus on the degree of hybridization. The general trend of the 3*d* Fe and Ni clusters to form compact structures in comparison with the 4*d* Ru and Rh clusters indicates a more metallic character in the bonding of the 3*d* ones and a tendency of a more covalent and directional bonding in the 4*d* ones. We have found that the number of *d* electrons relative to the *sp* ones is larger in the 4*d* clusters than in their isoelectronic 3*d* counterparts (see Tables I–IV). Due to the localized character of the *d* electrons by contrast to the delocalized *sp*, the bonding is expected in general to have more directional character in the 4*d* clusters, which have more *d* electrons than in the 3*d* clusters. In order to understand the origin of the larger per atom *d*-electronic charge relative to the *sp* charge in the 4*d* clusters as compared with the 3*d* ones, we have calculated—within an all-electron approximation of the DFT and using the same GGA functional and in both the nonrelativistic and the relativistic approximations—

TABLE II. Results for the different Ru_{13}, Rh_{13}, and Pd_{13} isomers as in Table I.

Structure	ΔE_B		μ	Dipole	*sp*	*d*	Distances	Bonds
Ru								
Cubic-T	0	(0)	0.15	0.44	0.87(0.86)	7.13(7.14)	2.48,2.29–2.69	26
Cubic-L	13	(13)	0.31	0.64	0.84(0.83)	7.16(7.17)	2.45,2.29–2.66	24
hcp	139	(149)	1.08	0.04	0.88(0.87)	7.12(7.13)	2.59,2.52–2.72	36
PP	181	(242)	1.69	0.03	0.85(0.88)	7.15(7.12)	2.63,2.47–2.71	37
ICO	209	(295)	1.54	0.02	0.85(0.88)	7.15(7.12)	2.67,2.56–2.72	42
BBP	219	(226)	0.46	0.31	0.87(0.86)	7.13(7.14)	2.58,2.47–2.71	36
Rh								
Cubic-L	0	(0)	0.69	0.29	0.86(0.83)	8.14(8.17)	2.49,2.42–2.66	24
Cubic-T	45	(46)	0.85	0.26	0.86(0.84)	8.14(8.16)	2.54,2.42–2.67	26
PP	53	(147)	1.31	0.03	0.82(0.82)	8.18(8.18)	2.67,2.56–2.87	37
ICO	63	(179)	1.62	0.00	0.82(0.83)	8.18(8.17)	2.73,2.63–2.76	42
hcp	67	(87)	0.92	0.07	0.82(0.83)	8.18(8.17)	2.64,2.58–2.81	36
BBP	81	(127)	1.15	0.20	0.82(0.82)	8.18(8.18)	2.66,2.56–2.85	36
Pd								
ICO	0	(37)	0.62	0.00	0.78(0.76)	9.22(9.24)	2.80,2.64–2.89	42
hcp	7	(0)	0.46	0.00	0.78(0.79)	9.22(9.21)	2.74,2.67–2.87	36
BBP	20	(11)	0.31	0.08	0.77(0.76)	9.23(9.24)	2.74,2.65–2.88	36
PP	28	(33)	0.62	0.00	0.79(0.77)	9.21(9.23)	2.76,2.66–2.95	37
Cubic-T	88	(130)	0.46	0.39	0.77(0.77)	9.23(9.23)	2.66,2.58–2.77	26
Cubic-L	105	(108)	0.39	0.31	0.78(0.78)	9.22(9.22)	2.62,2.57–2.74	24

the energy levels of the isolated atoms of Fe, Co, Ni, Ru, Rh, Pd in the $d^n s^1$ configuration ($n=7,8,9$ for Fe and Ru, Co and Rh, and Ni and Pd, respectively; this atomic configuration is the one closer to the electronic charge distribution calculated for the clusters). We have obtained the following trends which are illustrated in Fig. 4: (i) In the 3*d* atoms, without relativistic effects the Fe 4*s* level is slightly lower than the 3*d* one. Both are similar in Co, whereas the 3*d* is lower than the 4*s* in Ni. The relativistic effects separate the 4*s* levels from the 3*d* in Fe (and slightly in Co) and approach them in

TABLE III. Results for the different Fe_{23}, Co_{23}, and Ni_{23} isomers as in Table I.

Structure	ΔE_B		μ	Dipole	*sp*	*d*	Distances	Bonds
Fe								
PO-ICO	0	(92)	2.96	0.04	1.23(1.09)	6.77(6.91)	2.59,2.31–2.80	87
TW-ICO	22	(73)	3.13	0.06	1.26(1.08)	6.74(6.92)	2.58,2.44–3.01	82
EQ-ICO	62	(60)	2.96	0.01	1.23(1.09)	6.77(6.91)	2.57,2.34–2.94	82
hcp	79	(0)	2.96	0.13	1.21(1.09)	6.79(6.91)	2.55,2.31–2.78	76
EQ-PP	126	(41)	3.13	0.05	1.27(1.10)	6.73(6.90)	2.58,2.38–2.98	77
Co								
hcp	0	(25)	1.87	0.35	1.18(1.10)	7.82(7.90)	2.45,2.33–2.75	76
PO-ICO	15	(33)	1.87	0.02	1.17(1.10)	7.83(7.90)	2.50,2.30–2.65	87
EQ-ICO	33	(40)	1.96	0.21	1.20(1.10)	7.80(7.90)	2.48,2.34–3.00	79
EQ-PP	53	(0)	1.96	0.00	1.21(1.10)	7.79(7.90)	2.46,2.36–2.56	77
TW-ICO	60	(50)	2.04	0.01	1.21(1.09)	7.79(7.91)	2.49,2.36–2.65	81
Ni								
PO-ICO	0	(16)	0.78	0.01	1.15(1.12)	8.85(8.88)	2.50,2.31–2.69	87
EQ-ICO	14	(0)	0.61	0.00	1.12(1.11)	8.88(8.89)	2.49,2.34–2.86	82
EQ-PP	16	(14)	0.61	0.00	1.12(1.12)	8.88(8.88)	2.45,2.38–2.65	77
hcp	29	(31)	0.72	0.10	1.15(1.11)	8.85(8.89)	2.48,2.36–2.67	76
TW-ICO	46	(26)	0.78	0.01	1.14(1.11)	8.86(8.89)	2.49,2.32–2.86	82

TABLE IV. Results for the different Ru_{23}, Rh_{23}, and Pd_{23} isomers as in Table I.

Structure	ΔE_B		μ	Dipole	*sp*	*d*	Distances	Bonds
Ru								
Cubic	0	(0)	0.30	0.38	0.87(0.87)	7.13(7.13)	2.54,2.30–2.92	56
hcp	24	(23)	0.09	0.48	0.87(0.87)	7.13(7.13)	2.62,2.46–2.77	76
EQ-PP	43	(66)	0.26	0.25	0.89(0.87)	7.12(7.13)	2.61,2.40–2.95	70
EQ-ICO	71	(117)	0.35	0.31	0.88(0.87)	7.12(7.13)	2.62,2.29–2.95	70
TW-ICO	95	(109)	0.61	0.13	0.87(0.86)	7.13(7.14)	2.66,2.41–3.24	76
PO-ICO	141	(151)	0.69	0.02	0.87(0.84)	7.13(7.16)	2.68,2.51–2.79	87
Rh								
Cubic	0	(0)	0.39	0.15	0.85(0.84)	8.15(8.16)	2.57,2.44–2.82	54
EQ-PP	34	(22)	0.44	0.00	0.86(0.86)	8.14(8.14)	2.67,2.55–2.82	77
hcp	40	(51)	1.00	0.31	0.84(0.83)	8.16(8.17)	2.68,2.59–2.85	76
EQ-ICO	82	(67)	0.52	0.00	0.85(0.83)	8.15(8.17)	2.66,2.58–3.07	72
PO-ICO	96	(80)	0.31	0.02	0.82(0.81)	8.18(8.19)	2.72,2.53–2.92	87
TW-ICO	103	(90)	0.65	0.00	0.83(0.83)	8.17(8.17)	2.70,2.57–2.84	81
Pd								
EQ-PP	0	(20)	0.61	0.00	0.86(0.82)	9.14(9.18)	2.76,2.68–3.01	77
EQ-ICO	6	(8)	0.61	0.00	0.85(0.81)	9.15(9.19)	2.81,2.61–3.22	82
PO-ICO	6	(8)	0.35	0.00	0.77(0.77)	9.23(9.23)	2.82,2.58–3.00	87
hcp	7	(0)	0.13	0.11	0.79(0.79)	9.21(9.21)	2.76,2.68–3.04	76
TW-ICO	14	(17)	0.35	0.00	0.80(0.79)	9.20(9.21)	2.80,2.60–3.32	81
Cubic	61	(55)	0.13	0.18	0.81(0.81)	9.19(9.19)	2.70,2.57–3.07	60

Ni. (ii) In the 4*d* atoms, without relativistic effects the 4*d* level is always considerably lower than the 5*s* one. Relativistic effects in all cases approach the 5*s* and 4*d* levels. Besides, the relative difference between the 5*s* and the 4*d* levels increases from Ru to Pd. (iii) The change in the relative position of the *s* and *d* valence electrons due to relativistic effects is larger, as expected, in the 4*d* atoms than in the 3*d* atoms.

The electronic occupations reported in Tables I–IV correlate with the trends observed in the levels of the isolated atoms. The larger *d* occupation with respect to the *sp* one in the Ru, Rh, and Pd clusters than in their 3*d* counterparts is consistent with the 4*d* levels being at much lower energy with respect to the 5*s* than the 3*d* with respect to the 4*s* in Fe, Co, and Ni (larger *s* to *d* charge transfer occurs in the 4*d* than in the 3*d* systems). Besides, within the same row (either the 3*d* or the 4*d*) we have found that the *sp* occupation decreases as increasing the atomic number because the *d* valence level becomes lower and departs from the *s* level (an increase in the *s* to *d* charge transfer occurs as increasing the atomic number).

We have computed, for some selected isomers, the degree of hybridization between different orbitals by calculating the integral up to the Fermi level of the product of the corresponding orbital projected densities of states per atom. In Table V we compare the values of the *s*-*d* hybridization between paramagnetic 13-atom clusters in a compact (icosahedron) and an open [buckled biplanar (BBP)] structures. We find the *s*-*d* hybridization to be larger in the compact structure (ICO) than in the open one (BBP). Although the hybridization is also larger in the 4*d* clusters than in the 3*d* ones, there is not a clear relation between the *s*-*d* hybridization and the stability of a compact or an open structure. Thus, whereas in the 4*d* clusters of 13 atoms the BBP are more stable than

TABLE V. Results of the *s*-*d* hybridization for the ICO and BBP isomers of the 13-atom paramagnetic clusters.

3*d* element	Structure	*s*-*d* hybridization	4*d* element	Structure	*s*-*d* hybridization
Fe	BBP	1.23	Ru	BBP	1.29
Fe	ICO	1.47	Ru	ICO	1.67
Co	BBP	1.12	Rh	BBP	1.39
Co	ICO	2.08	Rh	ICO	2.18
Ni	BBP	1.19	Pd	BBP	1.32
Ni	ICO	1.72	Pd	ICO	2.20

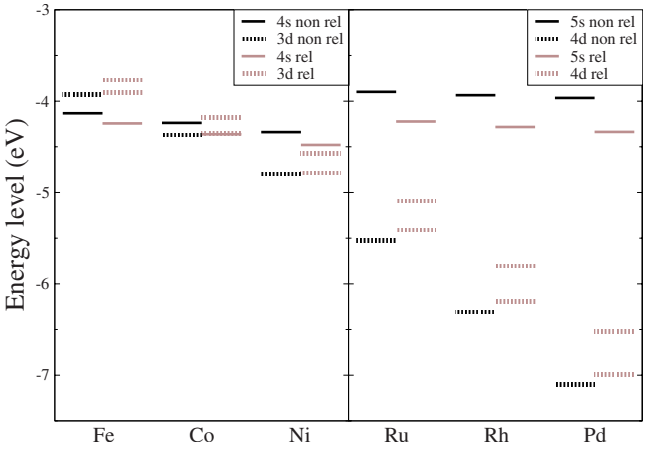

FIG. 4. (Color online) Electronic levels of the 3*d* and 4*d* isolated atoms in the nonrelativistic and relativistic approximations.

the ICO; in Co and Ni clusters the opposite situation is found. In Fig. 5 we plot the *s*- and *d*-projected density of states for the paramagnetic Fe_{13} and Ru_{13} clusters with ICO and BBP structures. The effective *d* bandwidth is larger for the BBP than for the ICO, and larger for Ru_{13} than for Fe_{13}. Although the *s* and *d* levels are farther apart in the 4*d* atoms than in the 3*d* ones, the larger bandwidth of the 4*d* states compared to the 3*d* ones makes 4*s*-3*d* and 5*s*-4*d* hybridizations comparable.

Concerning the similar average magnetic moment per atom in the 3*d* clusters of each element and size by contrast with the more dispersed values in their 4*d* isoelectronic counterparts, we start analyzing the magnetic couplings. All late 3*d* clusters exhibit parallel magnetic couplings reminiscent of their respective bulks. The values of the magnetic moments (about $3\mu_B$ in Fe clusters, $2\mu_B$ in Co ones, and a bit less than $1\mu_B$ in Ni) are consistent with the expected value if we assume the Hund's rule for the localized *d*-electron states, together with the transfer of typically one *s* electron to the *d* states due to the *s*-*d* hybridization, which takes place when going from the isolated atom to the cluster (see the per atom orbital occupations in Tables I and III) (somewhat smaller values in the respective bulks arise from the itinerant exchange). The 4*d* clusters, however, behave differently. Here, we notice that the respective bulks are paramagnetic, and therefore, although in the atomic limit one recovers the tendency toward magnetism, the spin polarization does not provide as much energy gain as in the 3*d* clusters. Besides, the *d* band results more occupied than in the 3*d* clusters and consequently, as expected for more than half-filled bands, the magnetic moments further drop. In the case of the Ru_{13} clus-

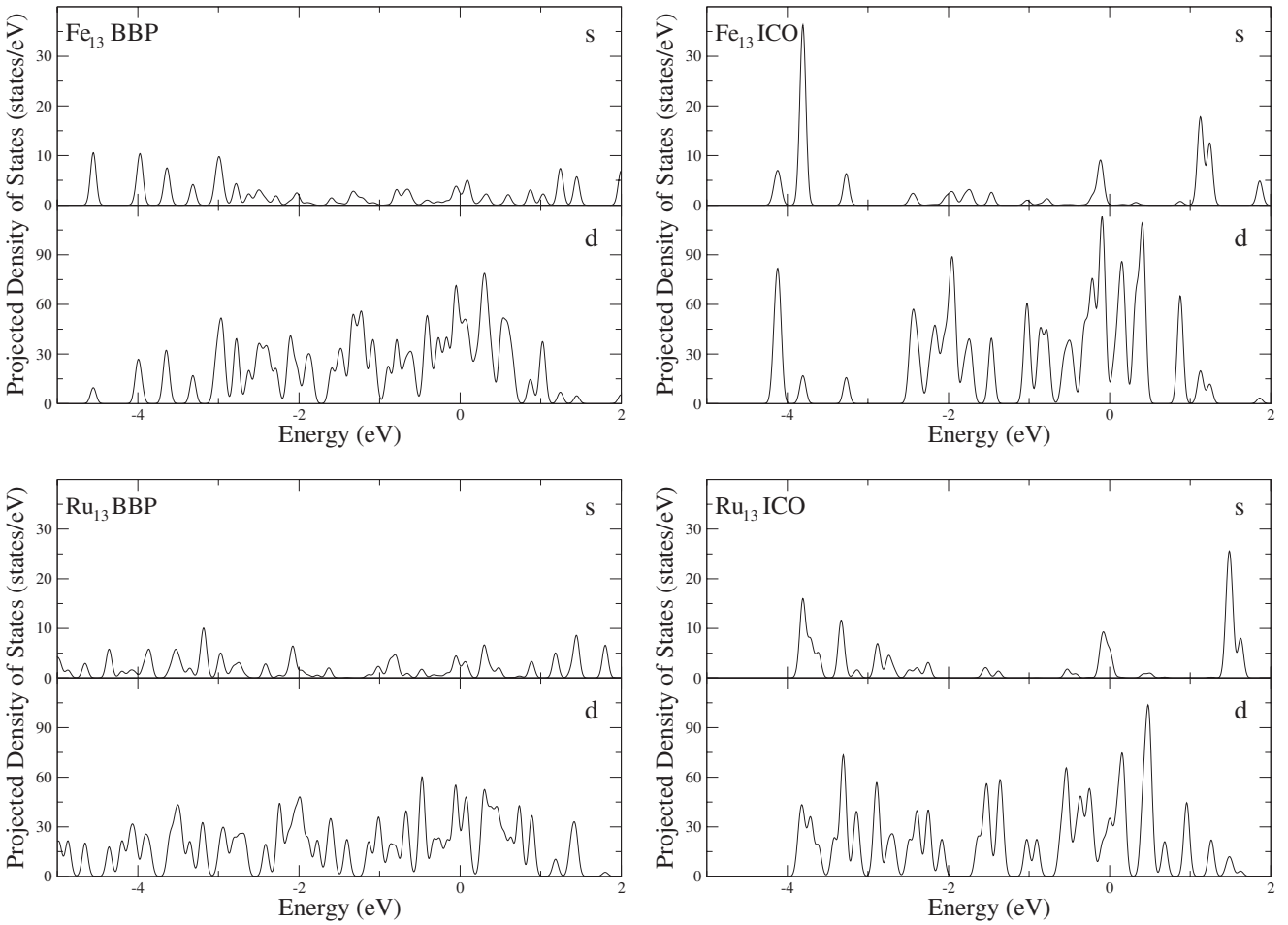

FIG. 5. *s*- and *d*-projected densities of states for paramagnetic Fe_{13} and Ru_{13} clusters with BBP and ICO structures. The energies are relative to the Fermi level.

ters, those isomers with the lower average magnetic moment (the cubic ones and the BBP) display certain degree of antiparallel magnetic coupling.

Whether the magnetism plays a role in the stabilization of the open or compact structures of these clusters is an interesting question that has to be addressed. We may shed some light on this through the comparison of the energetic order of the isomers in the paramagnetic state (notice that for each cluster we tested different spin arrangements, including the paramagnetic state) and looking for possible reordering with respect to the energetic order of the isomers in their most stable magnetic configuration. In Tables I–IV we have included for the paramagnetic state of each isomer, in parentheses, the total-energy difference with respect to the most stable paramagnetic one. Clearly magnetism is a driving force for the 3*d* Fe clusters. In Fe, when magnetism is switched off, the open structures result in being more stable than the compact ones, in contrast with the trend obtained when magnetism is considered. The tendency to compact structures in the magnetic case is consistent with the *d* to *sp* charge transfer associated to the spin splitting. The resulting average *d*-electronic occupation is typically reduced from 6.91 in the paramagnetic state to about 6.75 in the magnetic state. Then, the decrease in *d* electrons with respect to the *sp* works against the directional bonding, and thus, the magnetism works in Fe in favor of compact structures. In Ni clusters with few *d* holes available for spin polarization, magnetism is less important and the spin splitting does not change significantly the orbital occupancies so that in both the magnetic and the paramagnetic states their general tendency is toward compact structures. Co clusters are in between and no clear tendency is obtained from the calculations except their preference to stabilize in fragments of hcp-like symmetry (reminiscent of the structure of its bulk) over more compact structures, which is further favored by the magnetism.

In the case of the 4*d* Ru and Rh clusters, we have found that in the paramagnetic state there exists a correlation between stability and compacity of the structures, that is the less compact the structure of an isomer is, the more stable is this isomer in general (look at the energetic order and the total number of bonds). Also this trend does not change significantly when magnetism is switched on. Only for certain isomers an energetic order reverses. The magnetic moment in 4*d* clusters is lower than in the 3*d* ones, and the average orbital occupations in the 4*d* clusters are similar in both the paramagnetic and the magnetic configurations. Pd is also an exceptional case, in which the *d* states are close to be fully occupied. Many isomers are nearly degenerated for the 13-atom cluster and very close in energy for the 23-atom cluster. Pd_{13} clusters were studied recently by Wang and Johnson.[20] These authors concluded that Pd clusters do not prefer square-cubic order, but their structural habit is closer to noble metals than to other transition metals due to the complete filling of the *d* orbitals.

IV. SUMMARY

To summarize, we have presented a comparative study of the interplay between the electronic structure and the geometrical trends of the late isoelectronic 3*d* and 4*d* free-standing transition metal clusters. Compact structures are preferred by the 3*d* Fe and Ni clusters in contrast to the more open structures of the 4*d* Ru and Rh clusters, whereas Co and Pd clusters depart from the trend obtained in their respective 3*d* and 4*d* family. hcp structures are obtained for Co, whereas Pd does not prefer cubic structures but compact ones. A correlation is obtained between the tendency to form compact or more open structures and the relative *sp*- and *d*-electronic populations. The number of localized *d* electrons relative to the delocalized *sp* ones is larger in the 4*d* clusters than in their 3*d* counterparts, and more *d* electrons with less *sp* electrons favor the more covalent directional bonding of the cubic structures. The relative orbital occupations obtained in the clusters are consistent with the position of the energy levels of the respective isolated atoms, which play a role on the degree of *s*-*d* hybridization, although our results do not correlate the more open structures with larger *s*-*d* hybridization. Magnetism is found to play a role in the stabilization of the compact structures of the Fe clusters, which in general would have more open structures and more *d* electrons relative to the *sp* ones if they were nonmagnetic. Magnetism, thus, works in the 3*d* clusters in favor of compact structures, but its effect decreases as increasing the atomic number. Pd is a complex element whose clusters avoid cubic structures although the energy differences between most isomers are well below room temperature. The structural and magnetic trends of Pd clusters are still far from being completely understood.

ACKNOWLEDGMENTS

We acknowledge the financial support from PROMEP-SEP-CA230, CONACyT 2005-50650, by the Spanish Ministry of Education and Science (Project No. MAT2005-03415) in conjunction with the European Regional Development Fund and by the Junta de Castilla y León (Grant No. GR120). Computer resources from the Centro Nacional de Supercómputo (CNS) of the Instituto Potosino de Investigación Científica y Tecnológica (IPICyT), SLP, México, are also acknowledged.

[1] I. M. L. Billas, J. A. Becker, A. Chatelain, and W. A. de Heer, Phys. Rev. Lett. **71**, 4067 (1993).

[2] A. J. Cox, J. G. Louderback, S. E. Apsel, and L. A. Bloomfield, Phys. Rev. B **49**, 12295 (1994).

[3] F. W. Payne, W. Jiang, and L. A. Bloomfield, Phys. Rev. Lett. **97**, 193401 (2006).

[4] E. K. Parks, G. C. Nieman, K. P. Kerns, and S. J. Riely, J. Chem. Phys. **107**, 1861 (1997).

[5] A. Vega, J. Dorantes-Dávila, L. C. Balbás, and G. M. Pastor, Phys. Rev. B **47**, 4742 (1993).
[6] S. Bouarab, A. Vega, J. A. Alonso, and M. P. Iñiguez, Phys. Rev. B **54**, 3003 (1996).
[7] F. Aguilera-Granja, S. Bouarab, M. J. López, A. Vega, J. M. Montejano-Carrizales, M. P. Iñiguez, and J. A. Alonso, Phys. Rev. B **57**, 12469 (1998).
[8] F. Aguilera-Granja, J. L. Rodríguez-López, K. Michaelian, E. O. Berlanga-Ramirez, and A. Vega, Phys. Rev. B **66**, 224410 (2002).
[9] F. Aguilera-Granja, A. Vega, J. Rogan, W. Orellana, and G. García, Eur. Phys. J. D **44**, 125 (2007).
[10] Deng Kaiming, Yang Jinlong, Xiao Chuanyun, and Wang Kelin, Phys. Rev. B **54**, 2191 (1996).
[11] B. V. Reddy, S. K. Nayak, S. N. Khanna, B. K. Rao, and P. Jena, Phys. Rev. B **59**, 5214 (1999).
[12] D. Hobbs, G. Kresse, and J. Hafner, Phys. Rev. B **62**, 11556 (2000).
[13] O. Diéguez, M. M. G. Alemany, C. Rey, P. Ordejón, and L. J. Gallego, Phys. Rev. B **63**, 205407 (2001).
[14] V. Kumar and Y. Kawazoe, Phys. Rev. B **66**, 144413 (2002).
[15] B. V. Reddy, S. N. Khanna, and B. I. Dunlap, Phys. Rev. Lett. **70**, 3323 (1993).
[16] Deng Kaiming, Yang Jinlong, Xiao Chuanyun, and Wang Kelin, Phys. Rev. B **54**, 11907 (1996).
[17] C. M. Chang and M. Y. Chou, Phys. Rev. Lett. **93**, 133401 (2004).
[18] T. Futschek, M. Marsman, and J. Hafner, J. Phys.: Condens. Matter **17**, 5927 (2005).
[19] R. C. Longo and L. J. Gallego, Phys. Rev. B **74**, 193409 (2006).
[20] L. L. Wang and D. D. Johnson, Phys. Rev. B **75**, 235405 (2007).
[21] V. Bonacić-Koutecký, J. Burda, R. Mitrić, M. Ge, G. Zampella, and P. Fantucci, J. Chem. Phys. **117**, 3120 (2002).
[22] H. Hakkinen, M. Moseler, and U. Landman, Phys. Rev. Lett. **89**, 033401 (2002).
[23] E. M. Fernández, J. M. Soler, I. L. Garzón, and L. C. Balbás, Phys. Rev. B **70**, 165403 (2004).
[24] N. Agraït, A. L. Yeyati, and J. M. van Ruitenbeeck, Phys. Rep. **377**, 81 (2003).
[25] J. M. Soler, E. Artacho, J. D. Gale, A. García, J. Junquera, P. Ordejon, and D. Sánchez-Portal, J. Phys.: Condens. Matter **14**, 2745 (2002).
[26] N. Troullier and J. L. Martins, Phys. Rev. B **43**, 1993 (1991).
[27] L. Kleinman and D. M. Bylander, Phys. Rev. Lett. **48**, 1425 (1982).
[28] J. P. Perdew, K. Burke, and M. Ernzerhof, Phys. Rev. Lett. **77**, 3865 (1996).
[29] G. Rollmann, P. Entel, and S. Sahoo, Comput. Mater. Sci. **35**, 275 (2006).
[30] R. C. Longo, M. M. G. Alemany, A. Vega, J. Ferrer, and L. J. Gallego, Nanotechnology **19**, 245701 (2008).
[31] Q.-M. Ma, Z. Xie, J. Wang, and Y.-Ch. Li, Solid State Commun. **142**, 114 (2007).
[32] Z. Xie, Q.-M. Ma, Y. Liu, and Y.-Ch. Li, Phys. Lett. A **342**, 459 (2005).
[33] A. N. Andriotis and M. Menon, Phys. Rev. B **57**, 10069 (1998).
[34] Yang Jinlong, F. Toigo, and W. Kelin, Phys. Rev. B **50**, 7915 (1994).
[35] Y. C. Bae, H. Osanai, V. Kumar, and Y. Kawazoe, Mater. Trans. **46**, 159 (2005).
[36] Y. C. Bae, H. Osanai, V. Kumar, and Y. Kawazoe, Phys. Rev. B **70**, 195413 (2004).
[37] Y. C. Bae, V. Kumar, H. Osanai, and Y. Kawazoe, Phys. Rev. B **72**, 125427 (2005).
[38] W. Zhang, H. Zhao, and L. Wang, J. Phys. Chem. B **108**, 144413 (2004).